Smart Materials and Structures

PAPER • OPEN ACCESS

Ionic polymer-metal composite (IPMC) as a flexible capacitor: an experimental study

To cite this article: Liya Napollion and Kwang J Kim 2024 *Smart Mater. Struct.* **33** 125009

OPEN ACCESS
IOP Publishing
Smart Materials and Structures
Smart Mater. Struct. 33 (2024) 125009 (13pp)
https://doi.org/10.1088/1361-665X/ad8d95

Ionic polymer-metal composite (IPMC) as a flexible capacitor: an experimental study

Liya Napollion and Kwang J Kim*

Active Materials and Smart Living (AMSL) Laboratory Department of Mechanical Engineering, University of Nevada, Las Vegas (UNLV) 4505 S Maryland Pkwy, Las Vegas 89154, NV, United States of America

E-mail: kwang.kim@unlv.edu

Received 10 July 2024, revised 9 October 2024
Accepted for publication 31 October 2024
Published 7 November 2024

Abstract

In recent years, significant research has been directed towards the development of energy storage devices that are thin, lightweight, and flexible, catering to the diverse demands of modern smart electronics. This study investigates the remarkable adaptability of ionic polymer metal composite (IPMC) capacitors when subjected to bending conditions. Under investigation was the capacitor's functionality within a broad spectrum of bending angles, ranging from 0° to 100°. The study aims to reveal the capacitor's response and stability across this expansive curvature range, providing insights into its potential applications in flexible and dynamic systems. The flexibility of the supercapacitor allows it to bend or fold up to 180° without experiencing permanent mechanical deformation. The calculated specific capacitance values obtained by bending the cell at angles of 0, 40, 70, and 100° are found to be 4.3, 6.4, 8.2, and 8.4 mF g^{-1} respectively. The result displayed the IPMC capacitor exhibited notable resilience under varying bending angles, affirming its capacity to maintain operational integrity despite significant mechanical stress. Through a systematic exploration of bending conditions, this research unveils the capacitor's ability to flexibly conform to various bending angles. This adaptability is particularly significant for applications where traditional rigid capacitors may be impractical or inefficient.

Keywords: ionic polymer-metal composites (IPMCs), bending, supercapacitor, specific capacitance

1. Introduction

There is a significant growth in the industry of electrochemical energy storage devices, including batteries and supercapacitors [1–3]. Supercapacitors, also known as electrochemical capacitors, have gained popularity because of their unique properties including high power density, fast recharging capability, long cycle lifespan, simplified fabrication process, environmental friendliness, and enhanced efficiency, effectively closing the performance differences between batteries and capacitors [4–6]. They have been utilized across a spectrum of applications as energy sources for rapid energy storage and power delivery in consumer electronics, emergency power supplies, and wearable electronic devices [7–10]. Their phenomenal ability to bend, twist, and fold while displaying high capacitance, long-term cycling stability, and

* Author to whom any correspondence should be addressed.

compact features, ionic polymer metal composite (IPMCs) are promising candidates for next-generation patch devices [2, 11]. Despite their huge potential, flexible supercapacitors have encountered numerous issues. Among the main considerations for successful manufacturing of wearable flexible devices is maintaining highly stable mechanical and electrochemical performance under various deformations when the cell is bent at different angles under wet conditions [11, 12].

Furthermore, as current supercapacitors are still too bulky, heavy, and rigid to be practical for integration into wearable electronic devices, flexible supercapacitors must display a planar, compact design with minimal thickness, typically implementing a sandwich-type arrangement. While a wide range of materials have been investigated for supercapacitor applications, the field remains limited by the lack of suitable materials. In the past, carbon-based porous materials have been explored for the use in flexible supercapacitors. For instance, Kaempgen *et al* [13] manufactured thin film supercapacitors using single-walled carbon nanotubes (SWCNTs) in conjunction with a printable gel electrolyte. However, the promise of a highly flexible supercapacitor able to withstand bending and folding at lower cell voltage has yet to be attained. In this work, planar shaped ionic polymer-metal composite (IPMC) samples were fabricated utilizing platinum electrodes as the electrode material. The electrochemical performance of the IPMC supercapacitors under various bending angles was explored.

The internal structure of Nafion™ membrane in IPMC plays an important role in its electrochemical behavior. Nafion™'s structure consists of a hydrophobic fluorocarbon backbone and hydrophilic ionic clusters, which create microphase separation [14]. This separation results in the formation of interconnected ionic channels that allow for the movement of hydrated cations. The Gierke model, which describes the nanoscale structure of Nafion™, suggests that these ionic domains are approximately 3–5 nm in diameter and are responsible for ion conduction [15, 16]. As a result, the internal structure of Nafion™ has a direct influence on the charge storage capacity and transport behavior within IPMC. The formation of these ionic channels is essential for the efficient migration of cations, which contributes to the material's overall electrochemical performance.

When a voltage is applied across the electrodes, hydrated cations within the polymer matrix, such as Na^+, Li^+, or H^+, move through hydrophilic channels formed by the sulfonate (-SO^{3-}) groups in the Nafion™ backbone. This ion migration creates an electrical double layer at the electrode interface and results in the bending actuation characteristic of IPMCs. Research shows that the mechanical deformation and electrochemical performance of IPMC are directly linked to the ion transport mechanism, which is influenced by factors such as the applied voltage, ion species, and water content within the polymer matrix [17, 18]. Studies further highlight the importance of water content in influencing the mobility of ions, which in turn affects the electromechanical behavior of IPMC [19, 20]. The degree of hydration not only governs the extent of ion migration but also impacts the polymer's conductivity, as dry IPMC exhibits lower ion mobility and thus reduced electrochemical performance.

The working mechanism of ionic electroactive polymers (EAP) such as the IPMC requires electrodes like platinum, palladium, or gold through which an applied load polarizes the material, and consequently induces the movement of positive ions within the polymer membrane. Furthermore, the compact configuration of IPMC, illustrated in figure 1, shows the Nafion™ membrane sandwiched between two platinum electrodes. IPMC devices offer several benefits fundamental to ionic EAPs, including low driving voltages, flexibility, bidirectional movements, and relatively rapid actuation response times [21, 22]. Remarkably, the strain demonstrated by IPMC is similar to that of biological muscles and surpasses certain other artificial muscle actuators, such as shape memory alloys and conductive polymers [23].

Recent work investigates the potential of IPMC as planar and flexible capacitive elements for storing electrical energy [24, 25]. The study explored the electroactive abilities of IPMC capacitors including their dependance on temperature. The experiment considered dry (without water) IPMC samples, each sharing a uniform thickness but varying in surface area. A 5 nm chromium buffer layer was deposited on the polymer surface, ensuring strong adhesion between the 100 nm thick gold electrodes and the polymer membrane with a thickness of 127 μm. The electrochemical results exhibited capacitance values of approximately 1 mF cm^{-2} and a capacitance per unit mass of 40 mF g^{-1}. They were also successful in showing the rapid charging-discharging capabilities as it was shown in the results section of this work.

While the current work primarily focuses on the performance of IPMC in dry environments at room temperature, it is essential to distinguish that real-world applications will expose the material to a variety of environmental conditions, such as temperature fluctuations, varying humidity levels, and mechanical fatigue. These factors can significantly affect the long-term stability, reliability, and performance of IPMC capacitors. It is shown that higher temperatures affect the mechanical stability and conductivity of the membrane [26, 27]. Conversely, exposure to low humidity levels can lead to dehydration of the Nafion™ membrane, reducing ion conductivity and degrading performance [28]. Therefore, future work should involve testing the performance of IPMC strips under a wider range of environmental conditions, including variable humidity, temperature, and mechanical stress, to assess their suitability for real-world applications, especially in outdoor environments where they may be exposed to fluctuating conditions.

Additionally, mechanical fatigue tests are critical for evaluating the long-term durability of IPMC in flexible devices. Prolonged usage in bending or twisting applications can lead to microstructural fatigue or failure of the electrodes and polymer matrix. To address this concern, it is recommended that fatigue life and recovery behavior be studied in greater detail, particularly in relation to bending angles and cycles, as IPMC materials will likely be subjected to such mechanical stress in wearable or soft robotic applications. This will

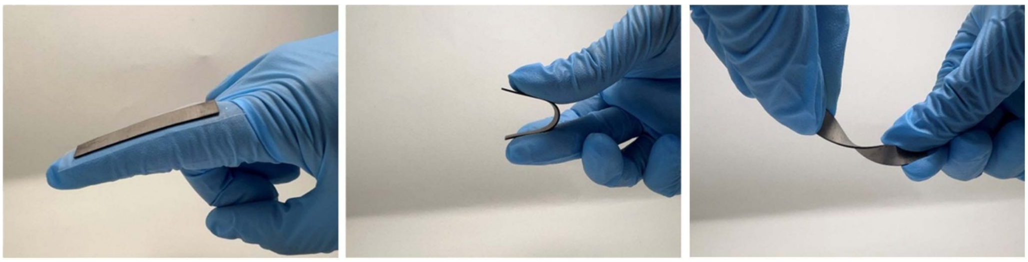

Figure 1. An IPMC capacitor, measuring 5 cm in length and 1 cm in width, designed for a wearable patch device showing neutral (left), bending (middle), and twisting (right) position, respectively.

offer a more accurate assessment of the material's practical applicability.

The findings of this study contribute to the evolving understanding of IPMC capacitor behavior, emphasizing its potential role in technologies that demand flexible energy storage solutions. The ability of the capacitor to endure and perform under diverse bending conditions makes it an attractive candidate for integration into systems where adaptability to complex shapes is essential. Moreover, the research suggests that IPMC capacitors can play a transformative role in shaping the future of flexible electronics and soft robotics. This investigation not only provides a broad understanding of the capacitor's performance under bending stress but also sets the stage for further research and innovation in the realm of flexible energy storage devices.

2. Experimental setup

2.1. IPMC fabrication process

The fabrication process of the IPMC comprises of numerous steps. In this work, impregnation-reduction process was used. A descriptive fabrication process is previously shown by Kim and Shahinpoor with performance comparison [29]. In addition, a more detailed electroless IPMC fabrication is also found from various research works [30, 31]. The basic fabrication process of IPMC begins with the preparation of the Nafion™ membrane. In order to improve the interfacial area and increase adhesion between the Nafion™ membrane and the electrodes, the surface of the membrane was roughened using sandpaper. To purify the membrane, it was immersed in hydrochloric acid and deionized (DI) water. The Nafion™ membrane is then placed in a platinum salt solution for four hours followed by sodium borohydride. Sodium borohydride is the reducing agent that metalizes platinum. The final step of the fabrication process is to soak the IPMC sample in a 1 M LiCl solution for cation exchange.

2.2. Scanning electron microscope (SEM)

Scanning electron images of the IPMC samples were developed utilizing the Hitachi TM3030 SEM operating at a 15 kV accelerating voltage. The image shows a smooth surface but nonuniform distribution of the platinum electrodes within the IPMC sample (figure 2).

2.3. Electromechanical universal testing machine

As seen in figure 3, a three-point bending load was applied to characterize the flexural stress-strain relationship of the fabricated IPMC samples under bending loading conditions. Young's modulus measurements were acquired from the stress-strain measurement utilizing the Instron 5565 Series. The strain rate was set to 0.5 mm min^{-1}. Multiple IPMC samples were tested, and each sample consisted of rectangular strips measuring 50 mm in length, 10 mm in width, and an average of 0.70 mm in thickness. Because of lack of control of the distribution of the platinum on the surface of the membrane during the fabrication, the thickness of the samples varies. It is important to note that the bending loading was conducted at room temperature ($\sim$23°) and humidity ($\sim$30%) in dry condition. It was noticed that residual moisture might still be present in the ambient environment or within the IPMC material itself, as it is always stored in DI water. This may potentially influence the ion mobility and measurement accuracy.

2.4. Setup for pneumatic-controlled bending test

Like flexible energy storage devices, the field of soft robotics has also been improving significantly in recent years [32]. Soft robots provide numerous advantages including flexibility, adaptability to diverse environments, ease of manufacturing, and enhanced safety in human-robot relations. For example, the finger-shaped actuator fabricated in this study displays the potential for handling softer objects without causing damage. In this study, the actuator plays an important role in controlling the curvature of the IPMC strips, as depicted in figure 4(c). The fabrication process starts with modifying the mold designs found from instructables.com (figure 4(a)), followed by 3D printing of the modified molds using thermoplastic polyurethane (TPU) filament (figure 4(b)). A mixture Dragon Skin^{TM} Pro Ecoflex is then prepared and poured into the molds. It is important to degas the mixture to eliminate air bubbles. Prior to filling, a small piece of fabric is placed in the bottom mold. The mixture was left to cure for approximately 4 h, after which the molded pieces are removed and joined together using Dragon Skin^{TM} Pro to create a single actuator unit.

2.5. Electrochemical characterization

The electrochemical responses of the prepared IPMCs were measured by PGZ-402 Potentiostat (Radiometer Analytical),

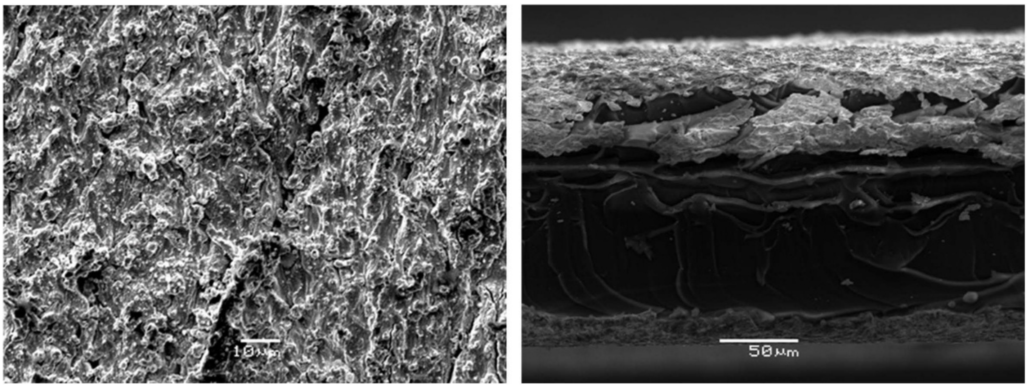

Figure 2. Cross-sectional SEM image of the IPMC before the application of mechanical loading, showing the platinum surface (left; reproduced from Napollion and Kim [21]) and the interface between the platinum surface and the nafion™ membrane (right). Reproduced from [31].

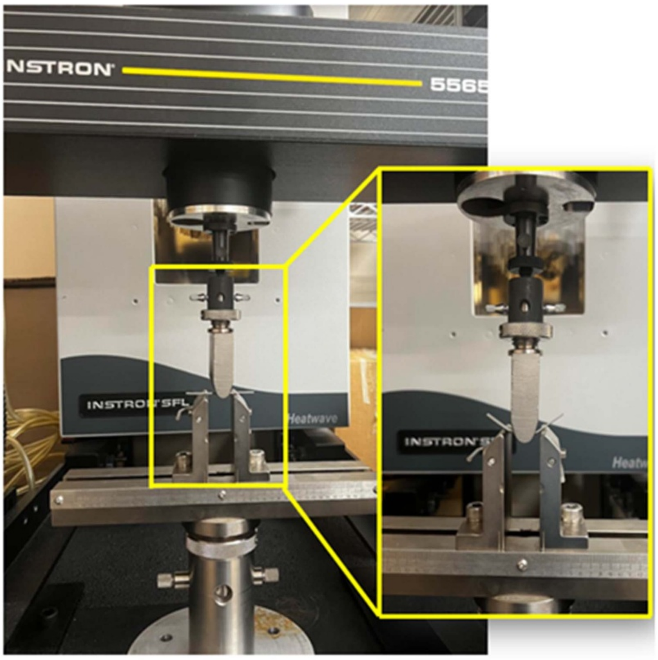

Figure 3. Three-point bending measurements of IPMC sample utilizing instron series 5565. The IPMC sample consisted of rectangular strips measuring 50 mm in length, 10 mm in width, and an average of 0.70 mm in thickness.

and Keithley (DMM6500) Multimeter. The cyclic voltammetry (CV) measurements were performed at a scan rate of 15 mVs^{-1} at room temperature ($\sim 23°$) using a two-electrode system. The electrochemical impedance spectroscopy (EIS) measurements were performed at a frequency range of 100 mHZ to 100 kHz. The curvature and pressure of the pneumatic actuator was controlled by a 100 ml syringe. Three IPMC samples with a size of 50 mm $\times$ 10 mm and thickness ranging from 0.70 mm to 0.75 mm were placed inside the soft actuator as shown in figure 5. The discharge specific capacitance (C_{sp}) values have been calculated from the CV curves of the chronopotentiometry measurements following equations (1)–(3),

$$C_{\text{sp}} = \frac{Q}{m\Delta V} \tag{1}$$

$$E = \frac{1}{2}\, C_{\text{sp}} V^2 \tag{2}$$

$$P = \frac{E}{\Delta t} \tag{3}$$

where Q is the average charge during the charging and discharging process, Δt is the discharge time window, ΔV is the potential window during discharging, and m is the mass of single electrode material. The energy density (E) and power density (P) are estimated using equations (2) and (3).

3. Results and discussion

3.1. SEM

The IPMC morphology was investigated by SEM. As displayed in figure 6(a), the IPMC displayed a relatively smooth surface with micro cracking around the edge. This change could be attributed to the mechanical stress from loading. The surface roughness has also increased because of the accumulation of stress-induced defects compared to figure 2. Elemental mapping was conducted to evaluate the distribution of the particles in cell as shown in figures 6(b) and (c). The homogeneous distribution of platinum and fluorine was confirmed by SEM-EDX.

3.2. Flexural stress-strain measurements

The flexural stress-strain measurement was conducted using the Instron 5565 Series. Under tension loading, it was reported that the mechanical strength of IPMC increases (both stiffness and the modulus of elasticity) relative to Nafion™; however, the overall performance still aligns with the intrinsic nature of Nafion™ itself [33]. Under the bending load, further increase

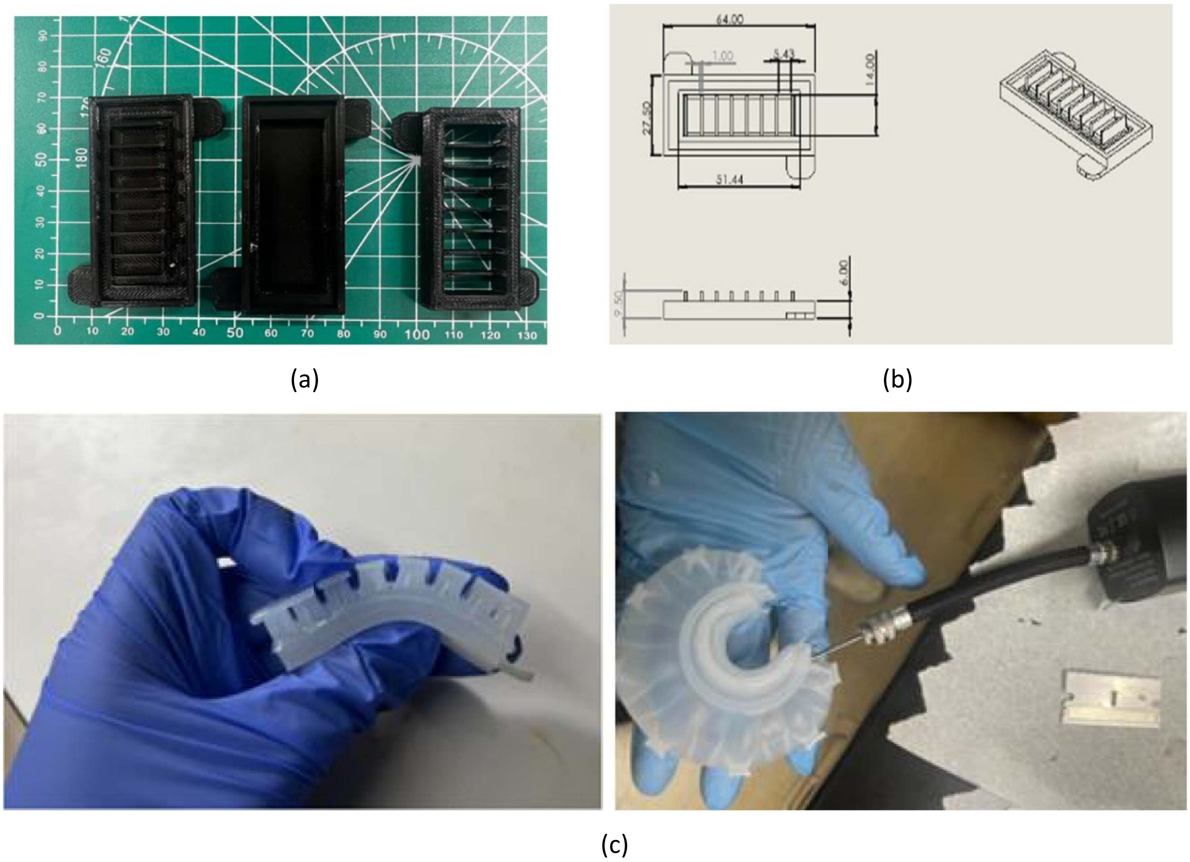

Figure 4. Modified pneumatic actuator mold design (original design was retrieved from instructables.com, www.instructables.com/soft-robotic-gripper/) (a), 3D printed of the actuator using thermoplastic polyurethane (TPU) filament (b), and the fabrication process of the actuator using Dragon Skin^{TM}FX pro ecoflex. parts A and B of the Dragon Skin were mixed and poured into molds. After curing, each part was sealed with Dragon Skin to ensure they were fully sealed and functional as pneumatic actuators (c).

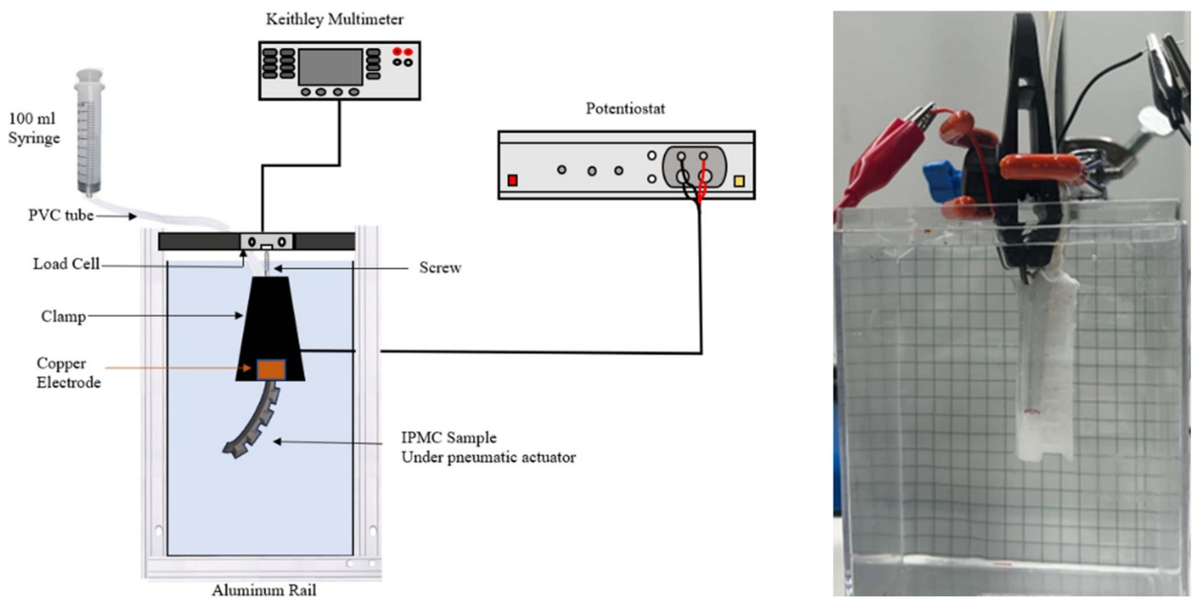

Figure 5. Experimental setup used for electrochemical characterization and corresponding schematic diagram using an IPMC measuring 5 cm in length and 1 cm in width. The measurements were conducted in DI water at a room temperature (∼23 °C). The electrochemical impedance spectroscopy (EIS) measurements were conducted in a two-electrode configuration at a frequency range of 100 kHz–100 mHz utilizing an AC perturbation of 10 mV. The photograph shows the test section where IPMC sample is inserted in a pneumatic actuator.

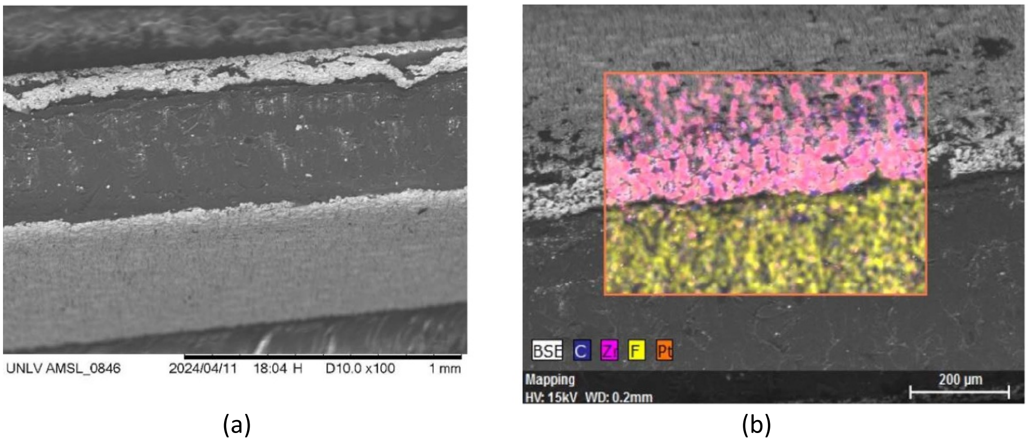

Figure 6. SEM image of the cross-section of the IPMC sample after 100 bending cycles (a) and an EDX analysis of the interface between the platinum and nafion™ membrane, displaying the distribution of platinum and fluorine (b).

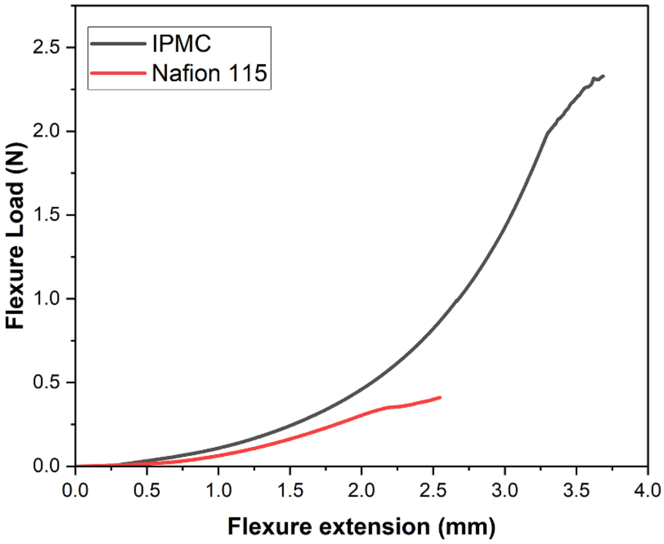

Figure 7. Flexural load-extension measurements of IPMC at a strain rate of 0.5 mm min^{-1}.

in both strength and flexural modulus for the IPMC, as illustrated in figure 7. The superior flexure load-extension performance of IPMC over Nafion™ can be attributed to the specific enhancements integrated into the IPMC. These enhancements include the incorporation of metal particles within the polymer matrix, which can offer additional mechanical integrity and improve the material's ability to withstand deformative stresses without compromising its elasticity. This makes the IPMC not only more resilient under mechanical loads but also better suited to applications requiring durable yet flexible materials.

3.3. Electrochemical measurements

3.3.1. Reproducibility. To explore the stability of the electrochemical performance of the IPMC capacitor and ensure reproducibility, a single IPMC sheet was fabricated and subsequently divided into five samples. From this, two samples were selected randomly for testing. Each sample measured 50 × 10 mm in length and width, with a thickness of 0.7 mm. For testing, the IPMC samples were immersed in DI water at room temperature. For the bending test, new IPMC samples were prepared using the same fabrication process as those shown for the reproducibility test. However, slight variations in thickness were observed because of the limitations in controlling the deposition of platinum on the surface of the polymer membrane during fabrication.

The two IPMC samples were characterized by utilizing CV test and the results display that the shapes of the two CV curves are similar, and their areas of the curves are close, displaying 3.4 mF g for sample 1 and 3.0 mF g^{-1} for sample 5. Figure 8 proves that the fabrication process for the IPMC samples shown in this study has a good reproducibility.

3.3.2. The electrochemical performance of the IPMC strips. The electrochemical charge storage behavior of the IPMC sample is studied in a two-electrode configuration using DI water as the electrolyte. To study the redox reactions occurring at electrode/electrolyte interface, CV measurements were performed, and the results are shown in figure 9. Figure 9(a) displays the cyclic voltammograms of IPMC in two-electrode configurations at various scan rates (15–100 mVs^{-1}). The CV plots displayed a quasi-rectangular shape, without any battery-like redox peaks suggesting the cell potential is varying linearly with time. In addition, the CV curves displayed symmetric characteristics with respect to voltage axis at zero current. This displays that the IPMC shows a close-to-ideal pseudo-capacitive electrochemical characteristics. Figure 9(b) displays the variation of the specific capacitance (C_{sp}) of IPMC with the scan rate calculated from the CV plots according to equation (1). The specific capacitance of the electrode material reached 3.4 mFg^{-1} at 15 mVs^{-1} and drops to 1.7 mFg^{-1} at a scan rate of 100 mVs^{-1}. Additionally, the chronopotentiometry curves measured at different current densities are depicted in figure 9(c). The nearly symmetric charge and discharge further validates the superior pseudo capacitance behavior of the electrode material in agreement with the CV

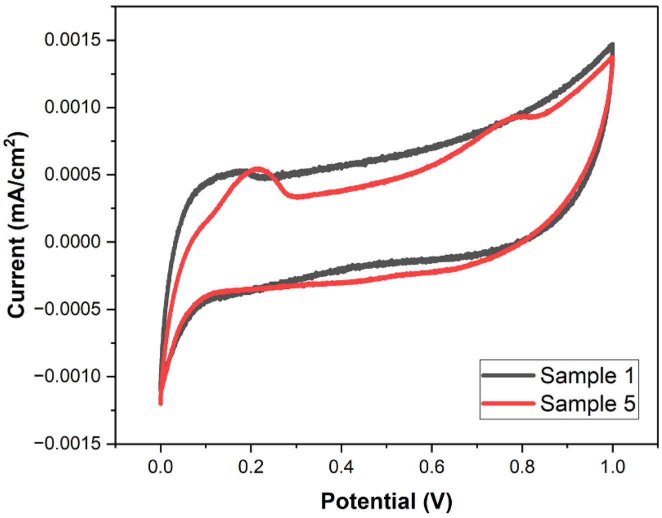

Figure 8. Cyclic voltammetry curves of two samples with the same conditions: The cyclic voltammetry (CV) measurements were performed at a scan rate of 15 mVs^{-1} in DI water at room temperature (∼23°), based on a two- electrode system.

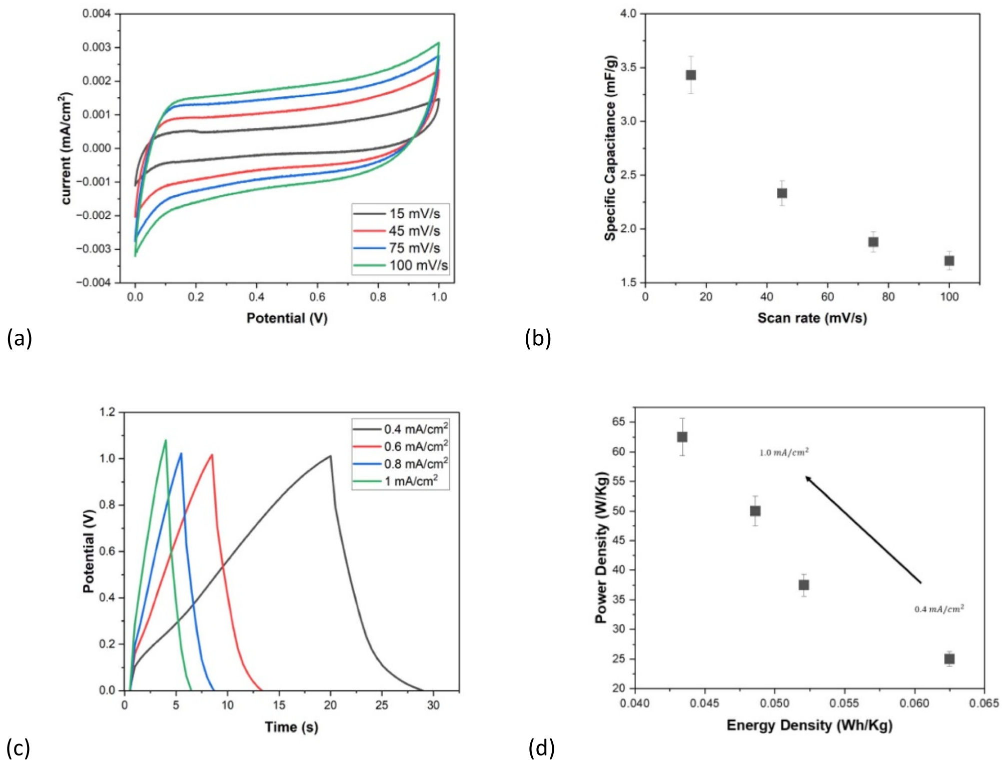

Figure 9. Cyclic voltammograms of IPMC in two-electrode configurations at various scan rates (a). Specific capacitance versus scan rates (b). Chronopotentiometry curves measured at various current densities (c) and their corresponding power versus energy density plot (d).

measurements. The lower current density of 0.4 $mA\,cm^{-2}$ displays a combination of capacitive electrode (triangular shaped) and faradaic electrode (plateau shape). Based on the chronopotentiometry, the energy (E) and power (P) density were calculated utilizing equations (2) and (3)), respectively, at various current densities. Figure 9(d) reveals the calculated energy and power density. At any current density, the values of E and P with C_{sp} values of the pt-IPMC electrodes are promising.

3.3.3. The electrochemical performance of the IPMC strips under bending condition. For the bending tests, new IPMC samples measuring 50 × 10 mm in length and width, with thickness ranging from 0.70 to 0.75 mm. The flexible supercapacitors are made into a wearable patch device acting as an electrochemical energy storage device, as shown in figure 1. The benefit of utilizing this flexible cell into wearable patch device is that it removes issues such as electrolyte leakage and electrode shorting during bending deformation as both

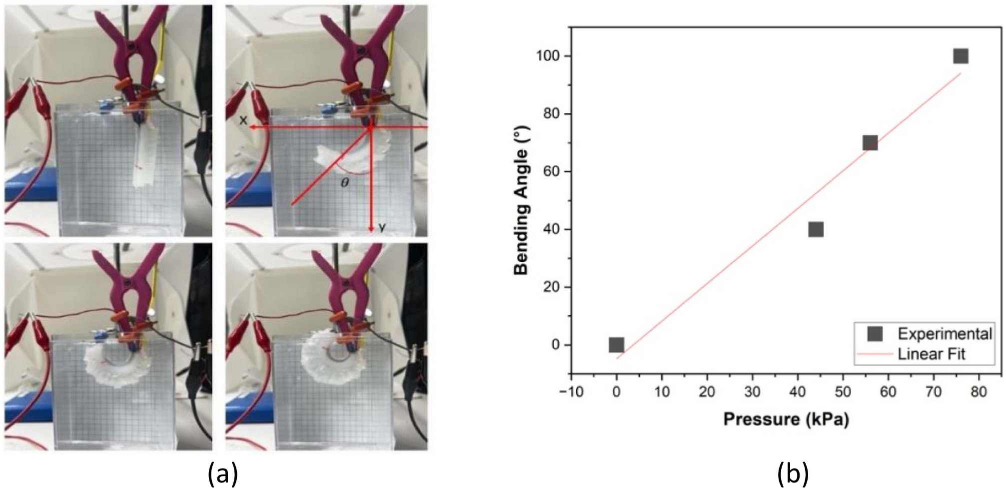

Figure 10. Experimental set up of the electrochemical performance of IPMC inside a pneumatic actuator (a). Pressure applied up to 80 kPa to control the curvature of the samples (b).

the electrode and electrolyte are super flexible and solid. The wearable patches were tested by placing the IPMC material inside a finger-like actuator as depicted in figure 10(a). The curvatures were controlled by a 100 ml syringe. The electrochemical performances of the samples were investigated by CV, EIS, and chronopotentiometry under various bending angles from 0° to 100°. At lower bending angle (0°), the pressure required to induce bending in the IPMC is relatively zero. This corresponds to the region where the IPMC undergoes little to small deformation as seen in figure 10(b). As the bending angle increases, the pressure required to maintain the desired curvature displays a steady increase. It is important to note that when conducting these measurements to consider the hydrostatic pressure exerted by the water in addition to atmospheric pressure. In the experimental setup, the water surrounding the IPMC samples exerts hydrostatic pressure because of its depth, which varies depending on the immersion depth and the density of the fluid. In general, as the depth of immersion increases, so does the hydrostatic pressure acting on the IPMC samples and the pneumatic actuator. However, in this case, the IPMC is placed near surface level, resulting in a small depth, thus rendering the hydrostatic pressure negligible. The total pressure can be calculated using equation (4),

$$P_{\text{total}} = P_{\text{atm}} + P_{\text{hydrostatic}} \tag{4}$$

where P_{atm} is the atmospheric pressure and $P_{\text{hydrostatic}}$ is the hydrostatic pressure.

When subjected to bending loading, the IPMC undergoes complex mechanical and electrochemical responses. Initially, at lower bending angles, the IPMC experiences minimal deformation, and the mechanical stresses are distributed relatively evenly across the sample. As the bending angle increases, the mechanical stresses on the IPMC become more pronounced, leading to deformation of the material as seen in figure 6(a). Deformation can cause changes in the microstructure and ion distribution within the material [33, 34]. This deformation can affect the distribution of water molecules and mobile ions within the polymer matrix of the IPMC, affecting its electrochemical properties. Figure 11(a) displays the CV curves of the strip IPMC supercapacitor measured at various bending angles, at the scan rate of 15 mVs^{-1}. It is observed that the shapes of the CV curves vary across different curvatures until reaching 70°. Beyond this point, the CV curves appear to exhibit slight change in the current response. This indicates there is no significant change for the capacitance of the strip supercapacitor beyond this position. As depicted in figure 11(b), the capacitance values calculated from the CV curves seem to increase with bending angle. Specifically, the capacitance values are recorded as 4.3, 6.4, 8.2, and 8.4 mFg^{-1} for bending angles 0°, 40°, 70°, and 100°, respectively. Studies also suggest that the capacitance and charge storage capacity of the IPMC tends to improve with bending angle [35]. In figure 11(c), the cycling stability of the cell is explored through the performance of 100 CV cycles. The result displays that the IPMC cell retains 100% of the initial specific capacitance up to 20 cycles. Then the cell retains an average capacitance of 99.5% throughout the duration of the measured cycle. In addition, in order to confirm the suitability of the flexible cell into wearable patch device, the change in the specific capacitance with respect to bending angles was conducted utilizing the chronopotentiometry cycles, as shown in figure 11(d). The measurements were conducted at a current density of 0.6 mA cm^{-2} by bending the cell at different angles. The flexible cell showed sustained high performance in DI water, remaining stable at 1 V. This voltage falls within the typical operating range of a standard wearable patch device, which typically works under 3 V operated at various bending angles [10, 36, 37]. The increase in the specific capacitance seen in the CV and chronopotentiometry curves can be attributed to several factors: enhanced ion transport, improved water uptake, and structural changes

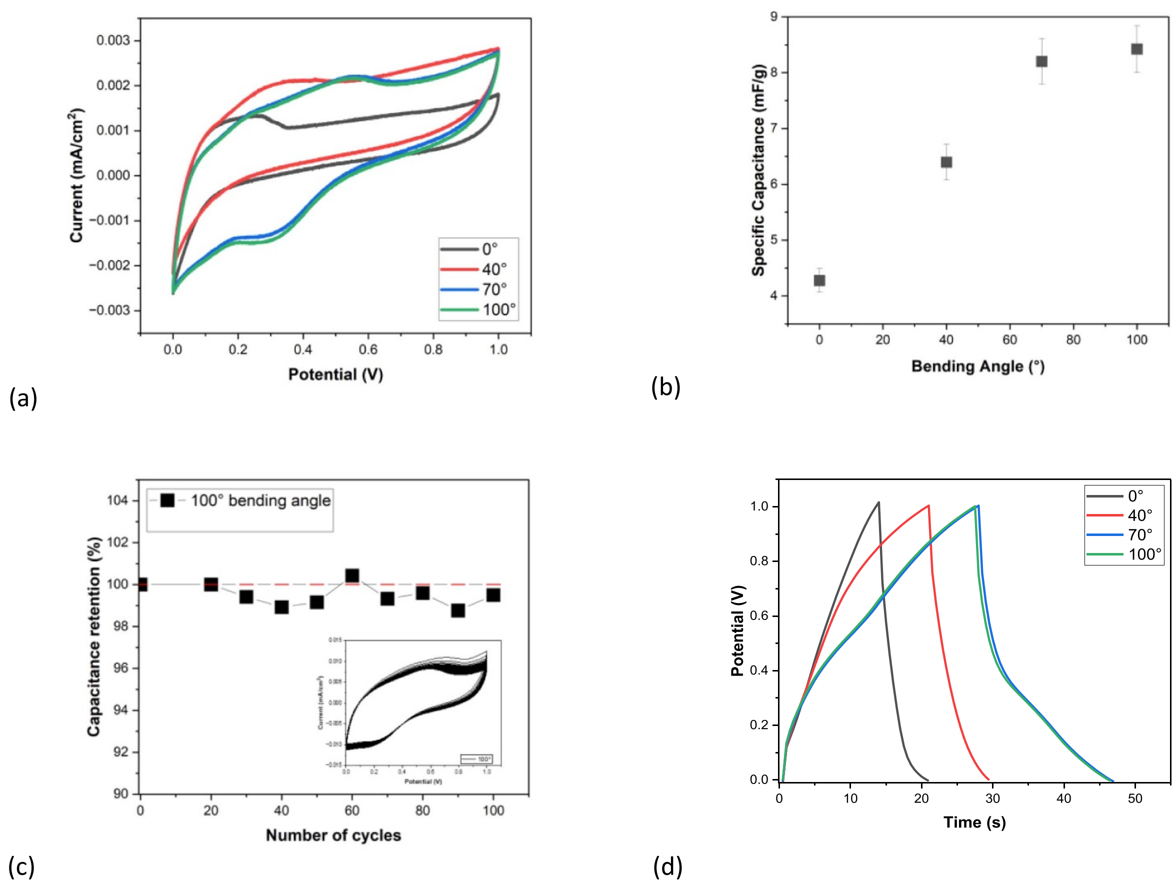

Figure 11. Cyclic voltammograms (a) obtained by bending the flexible IPMC samples at various angles performed at a scan rate of 15 mVs^{-1} and the corresponding specific capacitance measurements (b). The capacitance retention at various number of cycles (c), and the chronopotentiometry obtained by the flexible IPMC at various angles performed at current density of 0.6 $mA\,cm^{-2}$ (d).

within the material. The increased bending angle results in a larger surface area of the IPMC exposed to the surrounding electrolyte solution, leading to enhanced ion transport and electrochemical reactions at the electrode-electrolyte interface. Furthermore, mechanical deformation can facilitate the penetration of water molecules into the polymer matrix, enhancing the accessibility of ion exchange sites, therefore improving the electrochemical performance. In addition, the mechanical strain experienced by the IPMC may promote the reorientation of the polymer chains and the redistribution of charges within the material. This type of structural rearrangement contributes to the surface area of the electrodes and the availability of active sites for ion adsorption and desorption processes during oxidation-reduction process.

The IPMC cell underwent repeated bending to 100° followed by immediate restoration to the original flat state, mimicking its potential application in wearable patches. Notably, the measurements shown in figure 12 were conducted under bending conditions. Following bending and subsequent flattening of the IPMC samples 25, 50, and 100 times, specific capacitance values of 3.9, 3.8, and 4.0 mFg^{-1}, respectively, were observed. The observed increase in capacitance could potentially be attributed to enhanced contact between the platinum and Nafion™ membranes induced by external bending.

In order to investigate the variations in capacitance observed under various bending conditions, the impedance of the cell was examined through Nyquist plots within a frequency range of 100 mHz–100 kHz. Figure 13(a) displays the Nyquist plot of the free-standing IPMC strip. The equivalent circuit model was utilized for the EIS data simulation using ZSimpWin software (a free impedance analyzer) to get the fitting parameters. This equivalent circuit model was then applied to all Nyquist plots obtained under different bending conditions. Figure 13(b) depicts the Nyquist plots of the supercapacitor under various bending conditions. At higher frequencies, the equivalent series resistance (ESR) values of the IPMC strip under different bending conditions remained below 10 Ω-cm^2, obtained from the intercept of the Nyquist plots with the real axis. While there appeared to be slight fluctuations in the ESR values, it is crucial to note that ESR is primarily influenced by electrolyte resistance and contact resistance at the active material and current collector interface. Given the solid nature of the IPMC cell, the absence of electrolyte leakage implies stable electrolyte resistance by maintaining a consistent ion count within the electrolyte. Thus,

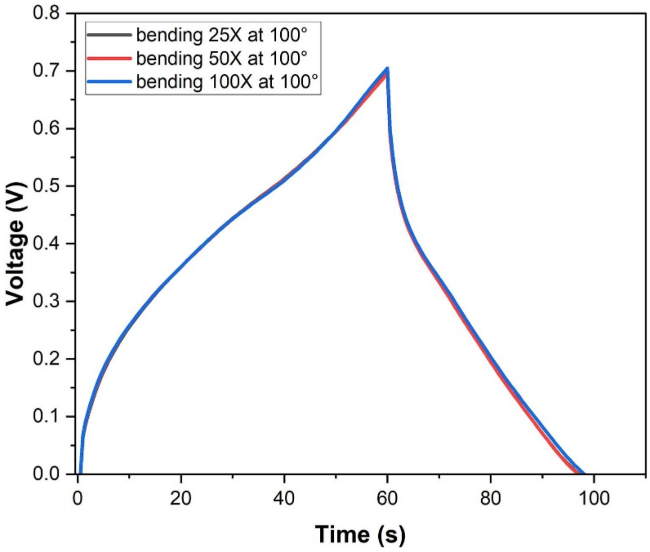

Figure 12. The chronopotentiometry data that was obtained by subjecting the flexible IPMC to bending cycles of 25X, 50X, and 100X at a bending angle of 100°, while maintain a constant current of 3 mA.

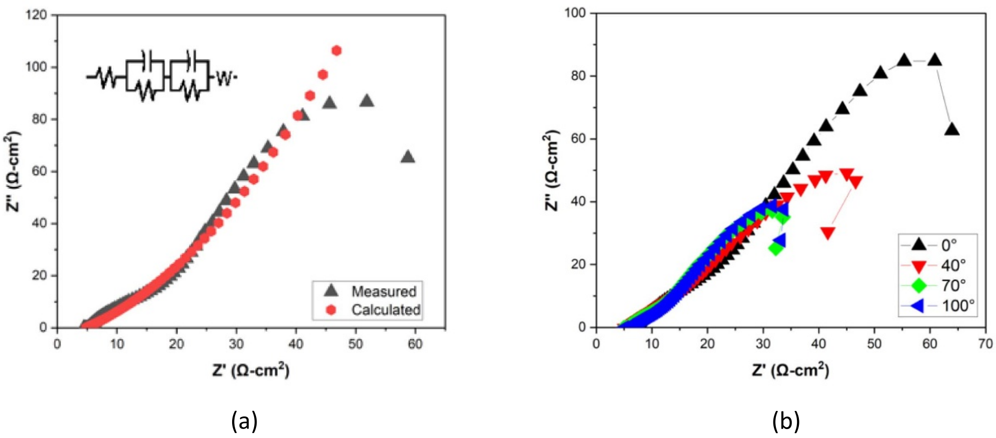

Figure 13. The EIS plot of the free-standing IPMC (a) and The EIS plots of IPMC strips under different bending conditions (b) measured at 0.5 V and room temperature within the frequency range 100 kHz–100 mHz.

any observed changes in ESR values are minor. Notably, an increase in bending coincided with a reduction in impedance magnitude, displaying an overall decrease in strip cell resistance. Such a decline in resistance often suggests diminished barriers to ion diffusion, facilitating enhanced ion mobility within the electrode-electrolyte interface. This enhanced ion diffusion can lead to more efficient charge transfer kinetics and electrochemical reactions, resulting in increased capacitance. On the contrary, an increase in resistance may indicate greater hindrance to ion diffusion, maybe because of high electrode polarization or poor conductivity of the polymer membrane. In such cases, the capacitance values decrease as a result of reduced ion mobility and slower charge transfer processes.

3.4. Application prospects and performance comparison

The reproducibility and bending tests conducted in this study provide key insights into the practical benefits of IPMC-based capacitors in flexible electronics. Specifically, the increase in capacitance with bending angle demonstrates that IPMC can maintain and even improve its electrochemical performance under mechanical strain. This is a particularly valuable characteristic for real-world applications, such as wearables and soft robotics, where devices are subjected to continuous mechanical deformation.

One of the most promising application areas for IPMCs is wearable electronics, where flexibility, durability, and the ability to conform to irregular surfaces are crucial. Wearable devices such as fitness trackers, smartwatches, and medical patches need energy storage systems that can operate effectively while being subjected to constant bending and movement. IPMCs are particularly suited for this because, unlike other flexible materials, their capacitance improves with mechanical deformation, as demonstrated in the bending tests performed in this study. The increased capacitance with bending ensures that energy storage performance remains stable or

(a) (b)

Figure 14. A red LED lit by a flexible IPMC charged for 30 s at 0.16 A at 0°(a) and 70° (b).

even improves during movement, which is essential for maintaining the functionality of wearables during daily activities. This characteristic prevents energy loss or device failure that might occur with more rigid materials under similar conditions. As a result, IPMC-based supercapacitors can provide more reliable power delivery, supporting devices that require long-lasting energy storage without performance degradation due to mechanical stress.

Furthermore, soft robotics is another field where IPMCs can play a significant role. Soft robots, designed to mimic biological organisms, often operate in environments that require them to flex, bend, and adapt to their surroundings. These robots rely on flexible energy storage systems that can accommodate complex mechanical deformations without compromising functionality. IPMC-based capacitors, with their ability to increase capacitance under bending, offer a significant advantage in this regard. Their capability to perform under various bending angles makes them an ideal energy storage solution for soft robotic systems that need to perform dynamic, repetitive motions.

Furthermore, IPMCs show several unique advantages over other flexible capacitor materials. For instance, graphene-based supercapacitors are known for their high conductivity and energy density, but they often face mechanical limitations under extreme bending or stretching, which can lead to performance degradation [38]. Similarly, while materials like polyaniline or polypyrrole offer good flexibility and conductivity, their performance under long-term mechanical deformation is often inconsistent, with significant reductions in capacitance over time due to structural breakdown [39]. For instance, in the work by Zhang *et al* the capacitance of the device dramatically decreased when bent to 30°, and further increases in bending angles to 60°, 90°, 120°, and 150° resulted in only slight changes in capacitance [6]. In contrast, the IPMC capacitors in this study demonstrated a substantial increase in capacitance, from 4.3 mF g^{-1} at 0° to 8.4 mF g^{-1} at a 100° bending angle. This highlights a significant advantage of IPMC capacitors in maintaining and even enhancing energy storage capacity under mechanical strain, making them more suited for flexible applications like wearable electronics or soft robotics. Moreover, the enhancement in capacitance under mechanical deformation could also reduce the need for larger or bulkier energy storage components in flexible systems. Since capacitance increases with bending, smaller or thinner IPMC layers could be used to achieve the same energy storage capacity as thicker materials in static conditions. This is particularly advantageous for miniaturized electronics, where space is limited, and energy efficiency is paramount. In addition, IPMCs' ability to operate in diverse environments, including humid or wet conditions, gives them an additional edge over other materials that may degrade or lose functionality in such environments.

Figure 14 displayed the practical application of an IPMC device in powering a red LED light under 0° and 70°, simulating conditions that might be encountered in wearable technology applications. For the setup, the IPMC was connected to a small red LED, which typically requires a voltage range of 1.7–3 volts to operate. The IPMC was initially charged with a current of 0.16 A at a voltage of 3 V for a duration of 30 s using a power supply. This charging protocol was chosen based on the electrical requirements of the LED and the capacity of the IPMC to store and deliver the necessary power efficiently.

Following the charging phase, the LED was then allowed to light using the stored energy in the IPMC. Under both (0° and 70°) conditions, the LED successfully lit for an average duration of 8 s. This showed IPMC capacitors' durability and flexibility as it maintained functionality even when bent at a 70° angle.

4. Conclusion

In this study, IPMC strips were successfully fabricated and characterized. A single IPMC sheet was fabricated and subsequently divided into five samples. The fabrication of the wearable patch consists of a polymer membrane (Nafion™) sandwiched between platinum electrodes. The benefit of utilizing this flexible cell into a wearable patch device is that it removes issues such as electrolyte leakage and electrode shorting during bending deformation as both the electrode and electrolyte are super flexible and solid. The wearable patches were tested by placing the IPMC material inside a finger-like pneumatic actuator. The results showed the fabrication process of IPMC has a good reproducibility. In addition, the fabricated strips were still functioning without shorting under bending conditions. Moreover, the capacitance values calculated from the CV curves seem to increase with bending angle. Specifically, the capacitance values are recorded as 4.3, 6.4, 8.2, and 8.4 mFg^{-1} for bending angles 0°, 40°, 70°, and 100°, respectively. The flexible supercapacitor exhibits remarkable cycling stability, making it suitable for integration into flexible energy storage devices and wearable electronics. This study demonstrates that the cell retains 100% of the initial specific capacitance for up to 20 cycles, followed by an average capacitance retention of 99.5% throughout the remainder of the measured cycle duration.

In short, the mechanical deformation of IPMC materials under bending loading from 0° to 100° causes changes in their electrochemical properties, resulting in an increase in capacitance as evidenced by CV and chronopotentiometry curves. These observations underscore the intricate interplay between mechanical strain and electrochemical behavior in IPMCs, highlighting the importance of understanding these phenomena for the design and optimization of IPMC-based devices in various applications.

Data availability statement

All data that support the findings of this study are included within the article (and any supplementary files).

Acknowledgments

This work was supported by the Department of Energy Minority Serving Institutions Partnership Program (MSIPP) managed by the Savannah River National Laboratory under BSRA Contract 0000525180. Also, we acknowledge the partial financial support from the US National Science Foundation (NSF), Partnerships for International Research and Education (PIRE) Program, Grant No. 1545857. Any opinions, findings, conclusions, or recommendations expressed in this material are those of the author(s) and do not necessarily reflect the views of the NSF. Additionally, L.N. thanks the generous financial support from the Howe Foundation Research Fellowships during her PhD study.

ORCID iD

Kwang J Kim https://orcid.org/0000-0003-2134-4964

References

[1] Dunn B, Kamath H and Tarascon J-M 2011 Electrical energy storage for the grid: a battery of choices *Science* **334** 928–35
[2] Kumar L, Boruah P K, Das M R and Deka S 2019 Superbending (0–180°) and high-voltage operating metal-oxide-based flexible supercapacitor *ACS Appl. Mater. Interfaces* **11** 37665–74
[3] Wang B, Liu J, Ock J, Motoyoshi R, Li S, Ueno K, Dokko K, Tsuzuki S and Watanabe M 2022 Lini0.5mn1.5o4-hybridized gel polymer cathode and gel polymer electrolyte containing a sulfolane-based highly concentrated electrolyte for the fabrication of a 5 V class of flexible lithium batteries *ACS Omega* **7** 17732–40
[4] Khedulkar A P, Dang V D, Thamilselvan A, Doong R and Pandit B 2024 Sustainable high-energy supercapacitors: metal oxide-agricultural waste biochar composites paving the way for a greener future *J. Energy Storage* **77** 109723
[5] Zhang J, Gu M and Chen X 2023 Supercapacitors for renewable energy applications: a review *Micro Nano Eng.* **21** 100229
[6] Zhang R, Xu Y, Harrison D, Fyson J and Southee D 2016 A study of the electrochemical performance of strip supercapacitors under bending conditions *Int. J. Electrochem. Sci.* **11** 7922–33
[7] Czagany M, Hompoth S, Keshri A K, Pandit N, Galambos I, Gacsi Z and Baumli P 2024 Supercapacitors: an efficient way for energy storage application *Materials* **17** 702
[8] Lu L, Zhang J, Xie Y, Gao F, Xu S, Wu X and Ye Z 2020 Wearable health devices in health care: narrative systematic review *JMIR mHealth and uHealth* **8** e18907
[9] Riaz A, Sarker M R, Saad M H and Mohamed R 2021 Review on comparison of different energy storage technologies used in micro-energy harvesting, WSNS, low-cost microelectronic devices: challenges and recommendations *Sensors* **21** 5041
[10] He Q, Yu M, Zhang X and Dai Z 2013 Electromechanical performance of an ionic polymer–metal composite actuator with hierarchical surface texture *Smart Mater. Struct.* **22** 055001
[11] Islam M R, Afroj S, Novoselov K S and Karim N 2022 Smart electronic textile-based wearable supercapacitors *Adv. Sci.* **9** 2203856
[12] Zhang Q, Gao X, Liu X, Mu J, Gu Q, Liu Z and Luo W 2024 Flexible wearable energy storage devices: materials, structures, and applications *Battery Energy* **3** 20230061
[13] Kaempgen M, Chan C K, Ma J, Cui Y and Gruner G 2009 Printable thin film supercapacitors using single-walled carbon nanotubes *Nano Lett.* **9** 1872–6
[14] Economou N, O'Dea J, McConnaughy T and Buratto S 2013 Morphological differences in short side chain and long side

chain perfluorosulfonic acid proton exchange membranes at low and high water contents *RSC Adv.* **3** 19525

[15] Costamagna P, Grosso S and Di Felice R 2008 Percolative model of proton conductivity of NAFION® membranes *J. Power Sources* **178** 537–46

[16] Liang Z, Chen W, Liu J, Wang S, Zhou Z, Li W, Sun G and Xin Q 2004 FT-IR study of the microstructure of nafion® membrane *J. Membr. Sci.* **233** 39–44

[17] Xian L, Li Z, Li S, Chen L and Tao W-Q 2023 Elucidating the impact mechanism of temperature and water content on thermal conductivity of hydrated nafion membranes by molecular dynamics simulation *Int. J. Heat Mass Transf.* **208** 124034

[18] Zhang H, Lin Z, Hu Y, Ma S, Liang Y, Ren L and Ren L 2023 Low-voltage driven ionic polymer-metal composite actuators: structures, materials, and applications *Adv. Sci.* **10** 2206135

[19] Lai J, Zeng B, Liu J, Zhang J, Pei W, Zhou Y, Liu Y, Li J and Tong Y 2024 Current research status of ionic polymer–metal composites in applications of low-voltage actuators *Mater. Adv.* **5** 4601–17

[20] Lee J H, Lee J H, Nam J-D, Choi H, Jung K, Jeon J W, Lee Y K, Kim K J and Tak Y 2005 Water uptake and migration effects of electroactive ion-exchange polymer metal composite (IPMC) actuator *Sens. Actuators* A **118** 98–106

[21] Park S, Kim S, Park S, Lee J, Kim H and Kim M 2022 Recent progress in development and applications of ionic polymer–metal composite *Micromachines* **13** 1290

[22] Ul Haq M and Gang Z 2016 Ionic polymer–metal composite applications *Emerging Mater. Res.* **5** 153–64

[23] Liang W, Liu H, Wang K, Qian Z, Ren L and Ren L 2020 Comparative study of robotic artificial actuators and biological muscle *Adv. Mech. Eng.* **12** 168781402093340

[24] Landrock C K and Kaminska B 2010 High temperature polymer capacitors for aerospace applications *2010 Design, Automation & Test in Europe Conf. & Exhibition (DATE 2010)*

[25] Lourenço L and Costa Branco P J 2015 Electric energy storage using ionic polymer metal composites: towards a flexible ionic polymer metal composite capacitor for low-power devices *Ionic Polymer Metal Composites (Ipmcs)* (Royal Society of Chemistry) ch 9, pp 286–333

[26] Avramov S, Lefterova E, Penchev H, Sinigersky V and Slavcheva E 2016 Comparative study on the proton conductivity of perfluorosulfonic and polybenzimidazole based polymer electrolyte membranes *Bulg. Chem. Commun.* **48** 43–50

[27] Gonçalves R, Tozzi K A, Saccardo M C, Zuquello A G, Barbosa R, de Oliveira Blanco G E, Hirano L A and Scuracchio C H 2024 Review on the use of impedance spectroscopy for IPMC-like devices: application, models, and a new approach to data treatment *Mater. Adv.* **5** 1817–45

[28] Bauer F, Denneler S and Willert-Porada M 2005 Influence of temperature and humidity on the mechanical properties of nafion® 117 polymer electrolyte membrane *J. Polym. Sci.* B **43** 786–95

[29] Kim K J and Shahinpoor M 2003 Ionic polymer-metal composites: II. Manufacturing techniques *Smart Mater. Struct.* **12** 65–79

[30] Pak J J, Cha S, Ahn H and Lee S 2001 Fabrication of ionic polymer metal composites by electroless plating of Pt *Proc. 32nd Intl. Symp. on Robotics* pp 19–21

[31] Napollion L and Kim K J 2023 Electrochemical performance of ionic polymer metal composite under tensile loading *Smart Mater. Struct.* **32** 095025

[32] Tauber F, Desmulliez M, Piccin O and Stokes A A 2023 Perspective for soft robotics: the field's past and future *Bioinspir. Biomim.* **18** 035001

[33] Lee S, Choi Y E, Lee J Y, Yang T, Jho J Y and Park J H 2023 Improved ionic and mechanical properties of ion-exchange membrane with an ionic silica network for high-performance ionic polymer-metal composites *J. Ind. Eng. Chem.* **122** 79–89

[34] Shahinpoor M, Bar-Cohen Y, Simpson J O and Smith J 1998 Ionic polymer-metal composites (ipmcs) as biomimetic sensors, actuators and artificial muscles—a review *Smart Mater. Struct.* **7** R15–R30

[35] Xu B, Wang S, Zhang Z, Ling J and Wu X 2021 Improving the torsion performance of IPMC by changing the electrode separation *Sci. Rep.* **11** 7639

[36] Pithadia S 2019 Improving battery life in wearable patient monitors and medical patches *Analog Des. J.* **1Q** (available at: https://www.ti.com/lit/an/slyt763/slyt763.pdf?ts=1730583009062)

[37] Low J-H, Chee P-S, Lim E-H and Ganesan V 2024 Kirigami-inspired self-powered pressure sensor based on shape fixation treatment in IPMC material *Smart Mater. Struct.* **33** 025029

[38] Zhang R, Palumbo A, Kim J C, Ding J and Yang E 2019 Flexible graphene-, graphene-oxide-, and carbon-nanotube-based supercapacitors and batteries *Ann. Phys.* **531** 1800507

[39] Chee W K, Lim H N, Zainal Z, Huang N M, Harrison I and Andou Y 2016 Flexible graphene-based supercapacitors: a review *J. Phys. Chem. C* **120** 4153–417